

2-2 Balloon-borne Superconducting Submillimeter-Wave Limb-Emission Sounder for Observations of Middle Atmosphere

IRIMAJIRI Yoshihisa

Recently, ozone destruction and global warming become serious problems. We are developing a balloon-borne superconducting submillimeter-wave limb-emission sounder (BSMILES) with a superconducting (SIS) receiver at 650-GHz band for observations of stratospheric ozone and other minor constituents that play important roles for ozone depletion. The sounder will be launched at Sanriku in 2003.

Keywords

Stratospheric ozone, Submillimeter wave, Superconducting receiver, Balloon-borne sounder

1 Introduction

We are currently developing a balloon-borne superconducting submillimeter-wave limb-emission sounder (BSMILES) for observations to determine the altitude profile of molecules affecting stratospheric ozone depletion. As shown in Fig.1(a), the limb sounding method allows the observation of the limb of the atmosphere in a tangential direction. Therefore, high-sensitivity observation is possible through deep penetration into the atmosphere; in other words, by employing a long distance of integration. The scanning of an observation beam at the elevation angle (altitude) provides high resolution in observation. The sounder receives emission line spectra from ozone and molecules relating to ozone depletion in the stratosphere to determine the quantity of these trace substances. Chlorine monoxide (ClO) is said to play an important role in the depletion of the ozone due to its interaction with chlorofluorocarbons. The intensity of emission lines from this molecule is weak in the millimeter band (200 GHz), while it is relatively strong in the sub-millimeter frequency band (650 GHz). In this band,

however, water vapor in the troposphere absorbs these molecules such that it becomes difficult to observe them from the ground (except for locations high in the mountains, at altitudes of thousands of meters). Observation from high altitudes thus requires the use of airplanes, balloons, satellites, or a space station. A manned airplane has advantages in controlling the arrangement of instruments and in repeated single-flight observations, but cannot reach altitudes that are high enough to enable observation of molecules with sufficiently high resolution. Observation from space is advantageous in that it becomes possible to observe a wide range of the earth's surface, although this method has the disadvantages of enormous costs in terms of development, time, and human resources. It is also necessary to take extensive precautionary measures before each launch. On the other hand, balloon-borne instruments are relatively cheap and can be developed using a small amount of resources in a short time. Moreover, if the balloon-borne instruments are designed to be recyclable, they can be used repeatedly, providing enough data to resolve problems and improve design. Thus, balloons

are often used to develop satellite-borne instruments. Compared with aircraft-borne instruments, balloon-borne instruments necessitate difficult measures to allow for operation in a vacuum, temperature control, and mechanical impact upon landing. These difficulties notwithstanding, balloons can reach the required altitudes, while airplanes cannot.

As for observations with millimeter- and submillimeter-waves using balloons, a balloon-borne microwave limb sounder (BMLS, Jet Propulsion Laboratory, USA) was used to measure O_3 and ClO using 200/270-GHz Schottky diode mixers[1][2]. Pointed infrared observation gondolas (PIROG 8, Sweden and France) performed observations of O_2 and O_3 using 425/441-GHz SIS mixers[3][4]. A submillimeter-wave limb sounder (SLS, Jet Propulsion Laboratory, USA) was used to measure O_3 , ClO, HCl, and HO_2 using Schottky diode mixers[5]. As for observations using aircraft, a family of submillimeter-wave atmospheric sounders (SUMAS, University of Bremen, Germany) was used to measure O_3 , ClO, HCl, HO_2 , and N_2O using 625-GHz to 650-GHz SIS mixers[6][7]. In Japan, no observations have been performed with submillimeter-waves using a balloon or airplane.

The first balloon launch is scheduled to take place at the Sanriku Balloon Center of the Institute of Space and Astronautical Science, Sanriku-cho, Kesenuma, Iwate-ken (at a latitude of 142 degrees east and 39 degrees north). Release of balloons will take place twice a year (in spring and in autumn) from this observatory. These balloons have no engines and will move with the prevailing winds, thus requiring favorable seasonal wind currents to permit controlled flight. Balloons will be launched when the air is calm—typically in the morning or evening. To observe ClO, the balloon will be launched in the morning, as this molecular component appears more often in the daytime. After launching, the balloon will move eastward by a westerly wind keeping a low altitude. After traveling about 100 km, ballast will be dropped so that the balloon reach an altitude of about 35 km in

the stratosphere. It will take 2 or 3 hours to reach the altitude. Then, it will change its direction and head west. Propelled by the easterly wind, it will travel westward at a speed of about 30 km/h. Its position will be determined using gondola-borne GPS instruments and a ranging telescope. When it arrives above the Pacific Ocean several tens of kilometers from the coast, we will send a command to cut the rope and to destroy the balloon. The gondola will then begin to fall, and an attached parachute will open. We will then use a helicopter or boat to recover the gondola. The observing time is approximately 5 hours. Since such landings on the ground are prohibited in Japan, the gondola must be waterproof if we wish to reuse it. The horizontal range of observation will be about 550 km at a tangent altitude of 10 km. Since the gondola will rotate in the azimuth direction (as no attitudinal control is necessary in this direction), the range of observation is a region within a radius of about 550 km around a center located off the coast of Sanriku Observatory. The districts of Southern Hokkaido, Tohoku, Kanto, and Koshinetsu are all within this range.

The center frequencies to be observed are as follows: 650.733 GHz for O_3 , 649.450 GHz for ClO, and 649.701 GHz for HO_2 , all in the submillimeter-wave band. Fig.1(b) shows a spectrum simulation of emission line spectra from these molecules at tangent altitudes of 15 km, 20 km, and 30 km.

2 Structure of the BSMILES System

Fig.2(a) is a block diagram of the BSMILES system. It comprises an antenna system, calibration system, optics system, receiver, IF system, spectrometer, data-acquisition and control system, attitude-detection system, and a power source. Fig.2(b) shows the expected construction of the BSMILES system. The gondola is W1.35 m \times L 1.35 m \times H 1.26 m (including height of I-bolt), weighs about 420 kg (including the ballast of 120 kg), and will consume approximately 140

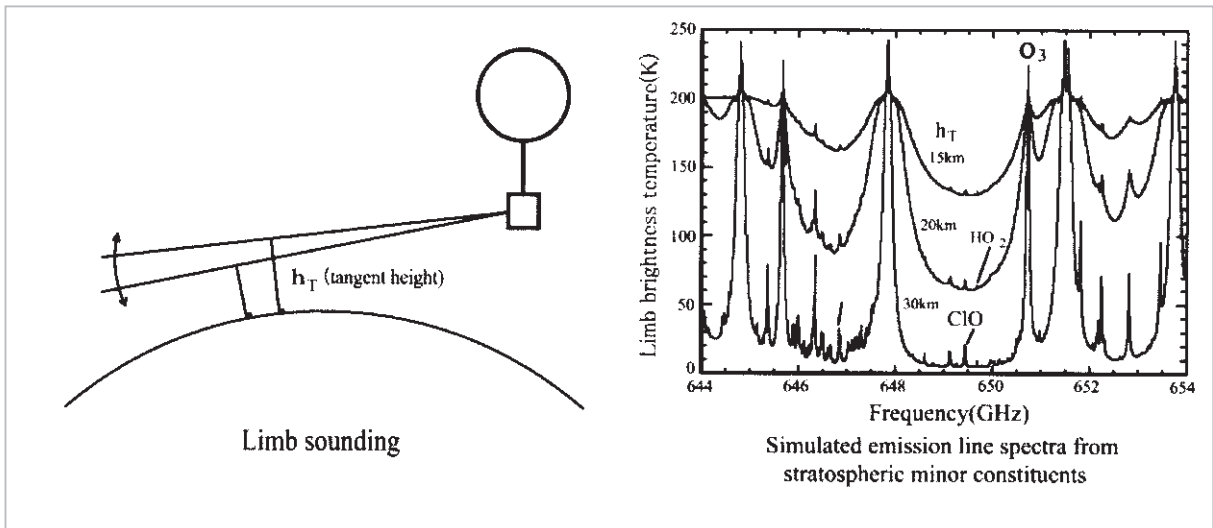


Fig.1 (a) Limb sounding method for observations of the atmospheric limb in the stratosphere—its advantages are that it has high-sensitivity and maximum height resolution observation capability (b) spectrum simulation of emission line spectra from O_3 (650.733 GHz), ClO (649.450 GHz), and HO_2 (649.701 GHz) at tangent altitudes of 15 km, 20 km, and 30 km

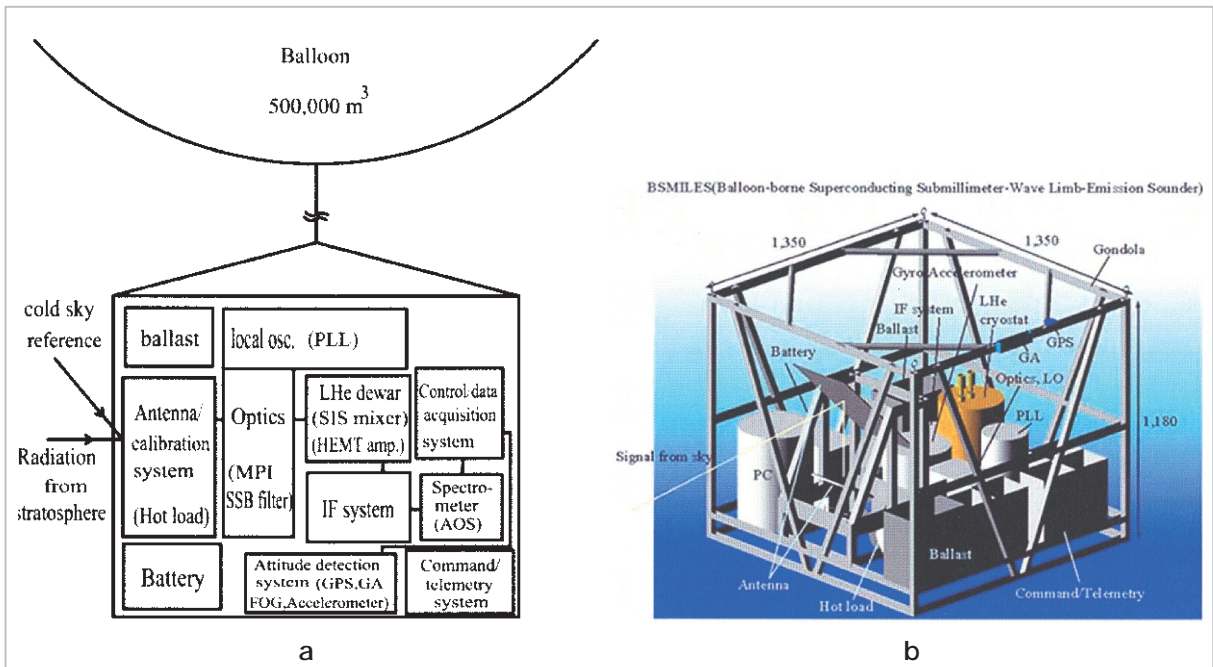


Fig.2 (a) Block diagram of the BSMILES system; (b) rendering of BSMILES

W of power. A gigantic balloon 100 m in diameter (about 500,000 m³) will be used to lift the structure to an altitude of 35 km. The gondola will be covered with polystyrene (100-mm thick) on all sides except for the signal window (about 650 mm in diameter). This material will enable the structure to float once it falls into the sea. The bottom of the gondola has pads to absorb the impact. Potential significant impacts include possible collision

with the stand owing to loose ropes at the time of a takeoff (about 30 G); acceleration at the time of a takeoff (about 2 G); impact on the sea surface (about 30 G); and impact during transportation (about 30 G). While the balloon is taking off, the gondola does not experience severe vibrations, as is the case with a rocket launch. Thus, instruments will be fixed in place with screws using spring washers and crash pads will be used to soften these

impacts.

2.1 Antenna System

The antenna system consists of an offset parabolic antenna (as the primary reflector) with an aperture of 300 mm, a sub-reflector, and a flat mirror (630 mm \times 350 mm) for beam scanning. The size of the beam from the parabolic antenna is about 0.1 degree, corresponding to an altitudinal resolution of about 1 km. The parabolic antenna is fixed, while the flat mirror is moved by a stepping motor to perform beam scanning for observation of the altitude profile of molecules in the direction of the elevation angle. Considering the altitudinal instability of the gondola, the beam is scanned in a range between - 8 and + 4 degrees, with an interval of approximately 20 seconds. At each scan, a flat calibration mirror (50 mm \times 50 mm) is moved to obtain calibration data through observation of the calibrated hot load and the cold sky at an elevation angle of 50 degrees. Launching of an ozone sonde[8] and a ClO sonde[9] with other balloons will serve to validate the observations, improving the final measurement accuracy to a target value of 10 percent.

2.2 Optics System

As shown in Fig.3, the optics system comprises a standing wave reducer, a Martin-Puplett interferometer (MPI) SSB filter, a sub-millimeter-wave local oscillator, a phase-locked loop (PLL) circuit, a local oscillator (LO) diplexer, and focusing mirrors. This system serves to measure the horizontal linearly polarized wave element (i.e., the half power) of randomly polarized observed signals.

Signals from the flat calibration mirror are reflected by the focusing mirror into a standing wave reducer. The reducer consists of a horizontal grid and a DC motor-drive movable roof mirror (with a stroke of about 2 and a vibration of about 10 Hz) that is slanted by 45 degrees. The roof mirror rotates a polarized wave by 90 degrees, which is then introduced by a focusing mirror into the MPI SSB filter. This filter consists of a 45-degree grid, two

fixed roof mirrors, a vertical grid placed before the mirrors (i.e., on the antenna side), and a cold load placed within a liquid helium cryostat. The mirrors are separated by 6.225 mm (for an IF of 6 GHz) from the 45-degree grid, to separate the upper sideband from the lower sideband. The separated upper sideband signals are introduced in the receiver, while signals in the separated lower sideband (image band) are terminated in the cold load. The targeted value of the separation ratio of the sidebands is 10 dB to 15 dB. Separated sideband signals are reflected by another focusing mirror through a local oscillator (LO) diplexer, and are then reflected by a focusing mirror (placed on a 4-K stage within the liquid helium cryostat) into a SIS mixer. A slightly slanted (from the horizontal to the vertical direction) wire grid is used as the LO diplexer. The ideal slope of the grid is determined so that the necessary minimum LO power (or a reflection coefficient of about 2 percent) may enter the SIS mixer. The LO signals are guided to the LO diplexer through a focusing mirror. Elements of the optics system are constructed in sizes that will allow an edge level of - 40 dB. As shown in Fig.4(a), the submillimeter-wave local oscillator consists of a Gunn oscillator, a doubler, a tripler, and a harmonic mixer for phase-locking. Its oscillating power is about 120 μ W at 644 GHz. The LO frequency is fixed at 644.220 GHz, and thus no other molecules are observable. This is a problem to be solved in the future. Stabilization of the LO phase lock and optimization of the oscillation output are very important in terms of observation. Since temperature variation has an effect on the oscillation output, the local oscillator is insulated thermally from the stand. A CPU is used to monitor and control the state of the phase lock so that when it becomes unlocked, phase will return to the locked state. We also plan to control the output from the oscillator.

As shown in Fig.4(b), the submillimeter-wave local oscillator and some elements of the optics system (including the SSB filter, the LO, the LO diplexer, and the focusing mir-

tank. A very low temperature variation and absence of mechanical vibration in the liquid helium cryostat contribute to the stability of the entire receiver system.

Porous Teflon (Zitex G108) 200- μm thick is used as an infrared filter, while Teflon (PTFE or PFA) 500- μm thick is used as a vacuum window. The transmission factor of Teflon is less than 5 percent at a submillimeter-wave band of 650 GHz. The vacuum window is attached at a Brewster angle that will reduce reflection. This window is also attached so as to align with a linear polarized wave (a vertical polarized wave signal when entering the cryostat) for observation. While the balloon is ascending through clouds and low-temperature regions, there is a risk that dew will form on the window and freeze, causing a loss in signal intensity. Thus, the window flange is covered with a sealed cylinder that is connected to the optics box. This structure prevents moisture from direct contact with the window, so that no dew may form on the cold window.

It is important to keep the liquid helium functioning properly during the experimental run. We found through experiment that the liquid helium tank is large enough to retain liquid helium for about 13 hours, as shown in Fig.5(b). This is longer than the specified

length of 10 hours, consisting of 5 hours of observation plus a reserve time of 5 hours (including the pre-launch preparation time and ascent time). In the above experiment, we measured the temperature of the 4-K stage after attaching a receiver to the 4-K stage, wiring the equipment, powering the amplifier, and attaching an infrared filter and the vacuum window.

It may be possible that more helium will be lost through the reduction in pressure during ascent, thus shortening the retention time. To prevent this from occurring, a pressure valve is attached to the liquid-helium filling port (and to the liquid-nitrogen filling port) to maintain the internal pressure at one atmosphere. On the other hand, a reduction in pressure further cools the SIS mixer (to 2 K), thus improving the capabilities and stability of the receiver. If the expected retention time is thus longer than required, it may be possible to conduct 2-K operations.

2.3.2 SIS Receiver

A superconductor-insulator-superconductor (SIS) mixer operating in the submillimeter-wave band (650 GHz) was designed and manufactured based on one for the 200-GHz band region[10]. As with other 200-GHz band devices, to produce a value of 4 for $R_n C_j$ (equaling a current density of 3.5 kA/cm²), we

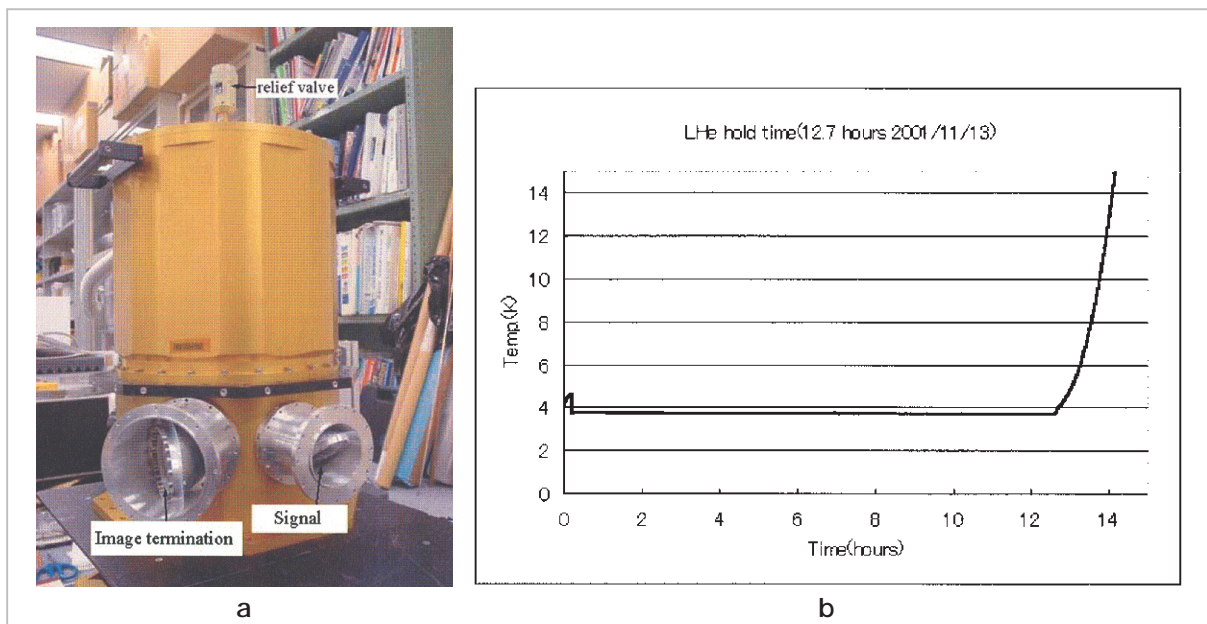


Fig.5 (a) liquid helium cryostat (b) measured retention time of liquid helium (about 13 hours)

have to construct an SIS junction of about 10 kA/cm² in current density. Since such a high-density junction leaks a large amount of current, it is difficult to construct one of high quality. Therefore, we set the value of $R_n C_j$ at 8 (designed with $R_n = 10.6$ and an SIS junction area of 1.56 μm^2). In this case, the current density is 5.5 kA/cm², making it easier to produce an SIS junction. Since the specific band is slightly narrow (12.5 percent), a deviation of the center frequency from the designed value lowers the performance in the required band. In a low-frequency band, such a problem would not occur, due to the relatively wider bandwidth. However, since in this case the center frequency depends on the junction area, care should be taken in constructing the SIS junction in question.

To cancel the junction capacity of the SIS junction, we constructed a parallel-connected twin junction (PCTJ)^{[11][12]}, using a method normally applied to join two SIS junctions by tuning inductance. A waveguide-type mount was used to the SIS mixer mount. A waveguide becomes quite small in the submillimeter-wave band, and it is difficult to construct a corresponding mechanical tuning mechanism. Thus, we used a tuner less mount that was fixed in position. A corrugated horn was used

as a feed horn. The SIS junction was made at the Nobeyama Radio Observatory at the National Astronomical Observatory of Japan. Nb/AlOx/Nb was used as a junction. Fig.6(a) shows an SIS junction joined to a mixer mount.

The noise temperature characteristics of an SIS receiver were determined by the Y-factor method. Fig.6(b) shows the measurement system in question. The system had a submillimeter-wave local oscillator (with an oscillation frequency range of 600 to 649.8 GHz) that consisted of a Gunn oscillator (with an oscillation frequency range of 100 to 108.3 GHz), a doubler, and a tripler. After being reflected by a focusing mirror, LO signals are introduced into the SIS mixer by 200- μm -thick Zitex G108 (porous Teflon (PTFE)). The transmission factor of Zitex G108 is about 2 percent in this frequency band. A mechanical cooler was used to cool the SIS mixer to 4.2 K. A 500- μm -thick Teflon (PTFE) was used as a vacuum window. A focusing mirror was placed on the 4-K stage with a reflection angle of 45 degrees to guide signals to the SIS mixer. A permanent magnet was used to reduce the Josephson current. A HEMT amplifier was placed on the 4-K stage and cooled to about 15 K. The intermediate fre-

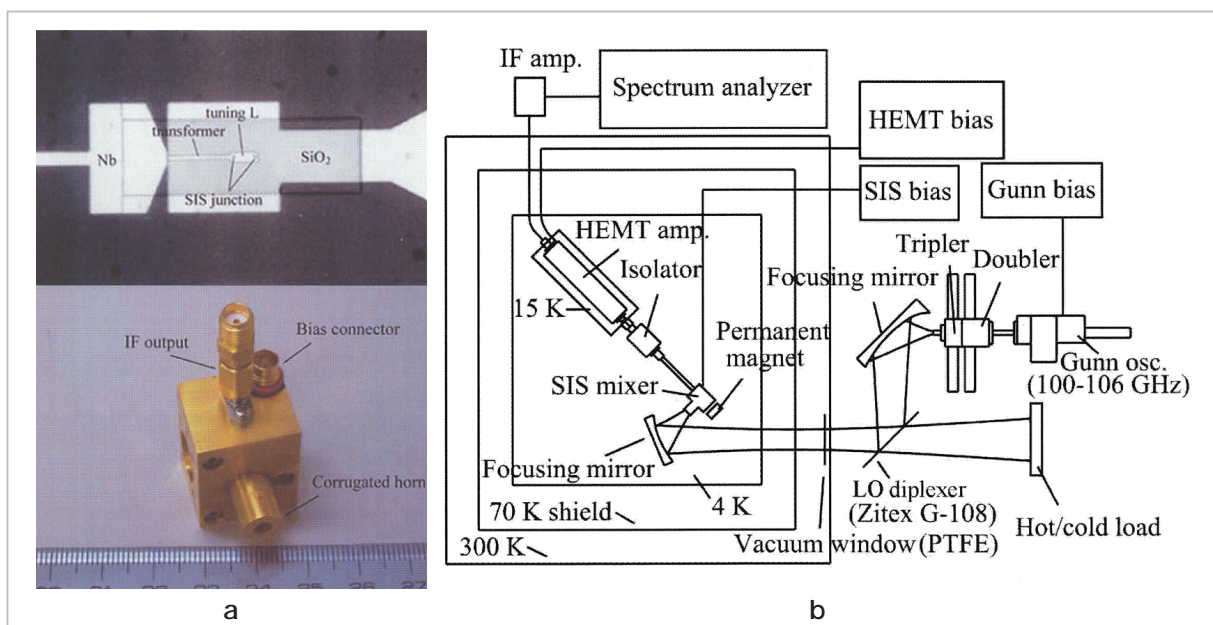


Fig.6 (a) PCTJ-type SIS junction (Nb/AlOx/Nb) and SIS mixer mount unified with a corrugated horn; (b) measurement set-up of noise temperature of an SIS receiver

quency was between 5 GHz and 7 GHz. The coaxial cable for use with the intermediate frequency had an external conductor of CuNi. The LO power and SIS bias voltage were optimized before measuring the Y-factor. An ambient-temperature IF amplifier (placed outside the cryostat) amplified the IF signals before measuring the Y-factor with a spectrum analyzer. In this measurement, the Y-factor was obtained as a ratio of output power from a hot load (radar absorber) at 300 K to that at 77 K (liquid nitrogen temperature). The receiver noise temperature calculated from this measurement includes not only the noise of the SIS mixer but also noise from the optics system and from the IF system. Fig.7(a) shows the DSB receiver noise temperatures obtained in the measurement. In the 650 GHz band used for observation of O₃ and ClO, these temperatures were between 150 K and 200 K.

Fig.7(b) shows measurements made using a Fourier transform spectrometer. The mixer with a PCTJ-type junction provided frequency responses in a range between 500 GHz and 700 GHz. The bandwidth of about 14 percent in this figure is in good agreement with the value estimated from the value of $R_n C_j$. There was no response below 375 GHz due to cutoff by the waveguide. A mixer having a distributed-junction (DJ) array element, which is designed to provide a wide band at a low current density [13], featured a band about 2.5 times as wide as that of a PCTJ-type junction.

Fig.8 shows an arrangement of compo-

nents of the receiver placed on a 4-K stage in a cryostat. Signals coming through a signal window (about 1" in diameter) and reflected by a focusing mirror are guided at a 45-degree angle to the SIS mixer. First, IF signals are amplified by a HEMT amplifier with an isolator and then taken out of the cryostat through an IF cable (made of CuNi and connected to the amplifier). A permanent magnet is used to reduce the Josephson current. The cryostat has another window about 2" in diameter, near which a cold load for use as an image terminator of the SSB filter is placed on the 4-K stage. A temperature sensor is attached to the 4-K stage to measure temperatures around 4 K. Another sensor is attached to the HEMT amplifier to measure its temperature. The HEMT amplifier is attached with an aluminum plate to the 4-K stage. Experiment revealed that the amplifier was cooled to a steady-state temperature of about 14 K. The frequency range of the amplifier is 5 GHz to 7 GHz, gain is 30 dB or more, gain deviation is ± 1.5 dB or less, input equivalent noise temperature is 18 K (a standard value, including noise from the isolator), and input VSWR is 1.4 (standard value).

2.4 Intermediate Frequency System

Taken out of the cryostat, signals are guided through an IF cable (made of Cu) to the intermediate frequency (IF) system. In this system, a power divider divides an initial IF signal (5 to 7 GHz) into two series of signals.

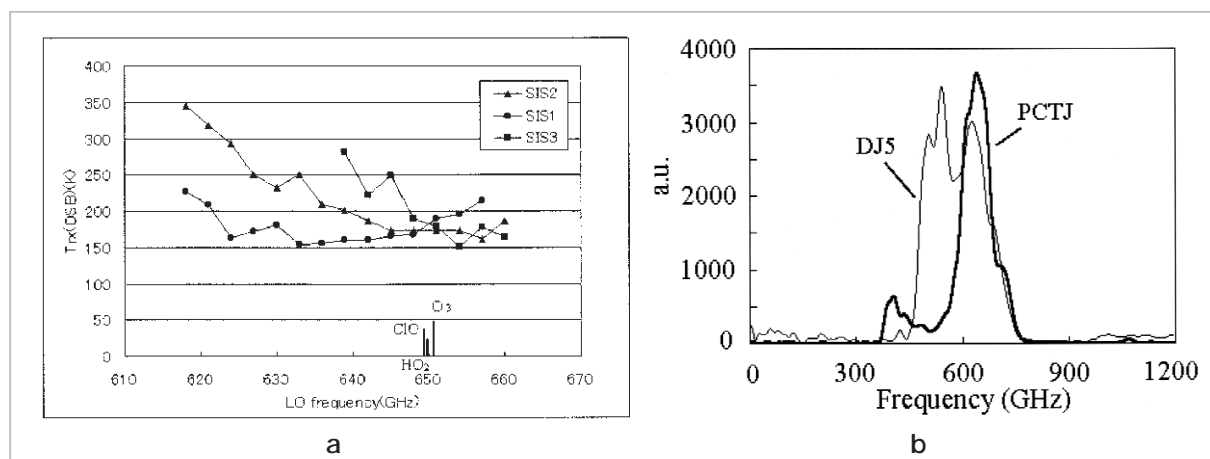


Fig.7 (a) DSB noise temperatures of an SIS receiver; (b) measurements using a Fourier transform spectrometer

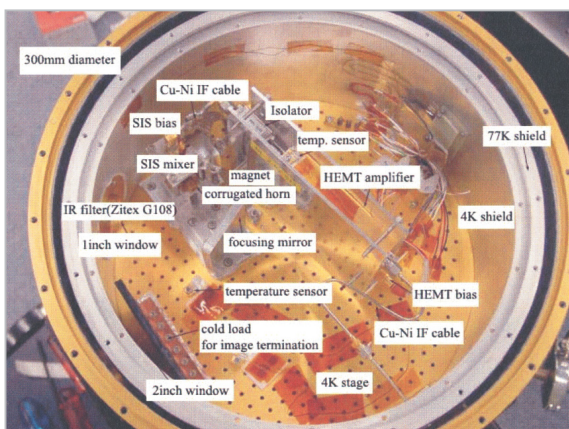


Fig.8 Arrangement of components of the receiver in a cryostat

The cryostat is placed upside-down with the cover removed (refer to Fig. 5).

For each series, a bandpass filter sorts signals either as first-band signals (5.03 to 5.53 GHz for ClO and HO₂) or as a second-band signals (6.313 to 6.813 GHz for O₃). Each of the bands is amplified by two amplifiers. Then, for each band, a second local oscillator and mixer convert the band into a second IF signal, which is amplified by an amplifier with a bandpass filter, and an isolator. Finally, these bands are combined and output into a spectrometer. The second LO frequency is 3.430 GHz and 4.213 GHz for the ClO/HO₂ band and O₃ band, respectively. These values are determined such that they can be converted to second IF signals within the spectrometer-treatable band (1.6 to 2.6 GHz). The final bands are 1.85 GHz \pm 250 MHz (with a bandwidth of 500 MHz) for ClO and HO₂ and 2.35 GHz \pm 250 MHz (with a bandwidth of 500

MHz) for O₃. A CPU-controlled switch outputs a comb generator signal (at a step frequency of 100 MHz) to calibrate the frequency used by the spectrometer. The total gain of the IF system is about 60 dB, which can be changed by attaching a fixed attenuator to the output side of each band. Fig.9(a) and 9(b) illustrate the structure of the IF system and the division and combination of bands.

2.5 Spectrometer

We used an acousto-optical spectrometer (AOS), as shown in Fig.10(a). The bandwidth is 1 GHz with a resolution of 1 MHz. One spectrum holds about 6.9 kByte of data with an integration time of 100 milliseconds for raw data. Table 1 shows the specifications for the spectrometer. A measured absolute stability of the Allan variance is about 200 seconds, as shown in Fig.10(b). A larger spectrometer bandwidth will be necessary to observe more species of molecules across a spectrum widened due to pressure broadening.

2.6 Data Acquisition and Control

The system for data acquisition and control has two CPUs. CPU 1 operates at a clock frequency of 66 MHz with a RAM of 16 MB under MS-DOS Version 5. The CPU 1 unit features the following boards, connected to an ISA bus: (i) a digital I/O board to acquire molecular spectrum data from the acousto-optical spectrometer; (ii) an RS232C board to acquire attitude data from a fiber-optical gyro-

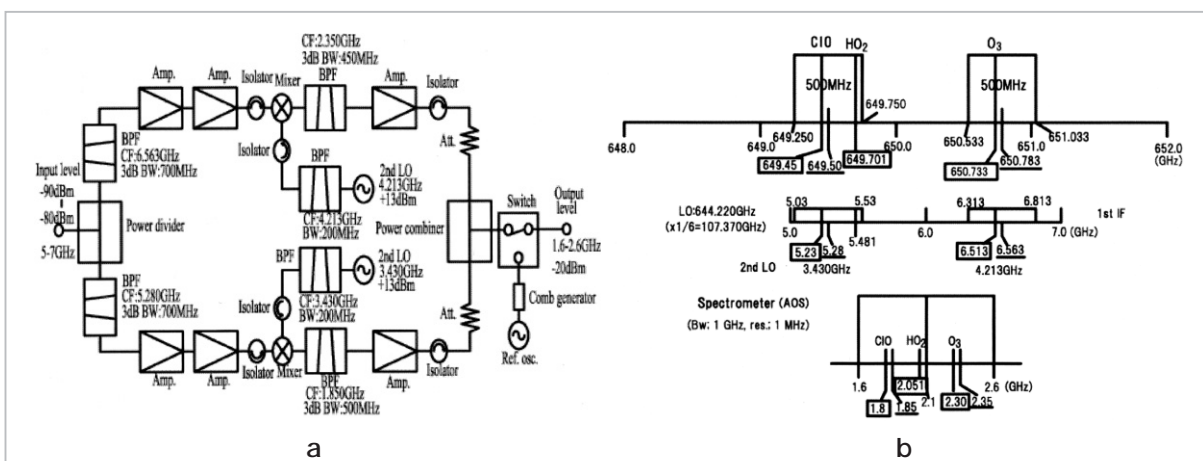


Fig.9 (a) Block diagram of the IF system; (b) division and combination of bands for ClO/HO₂ and O₃

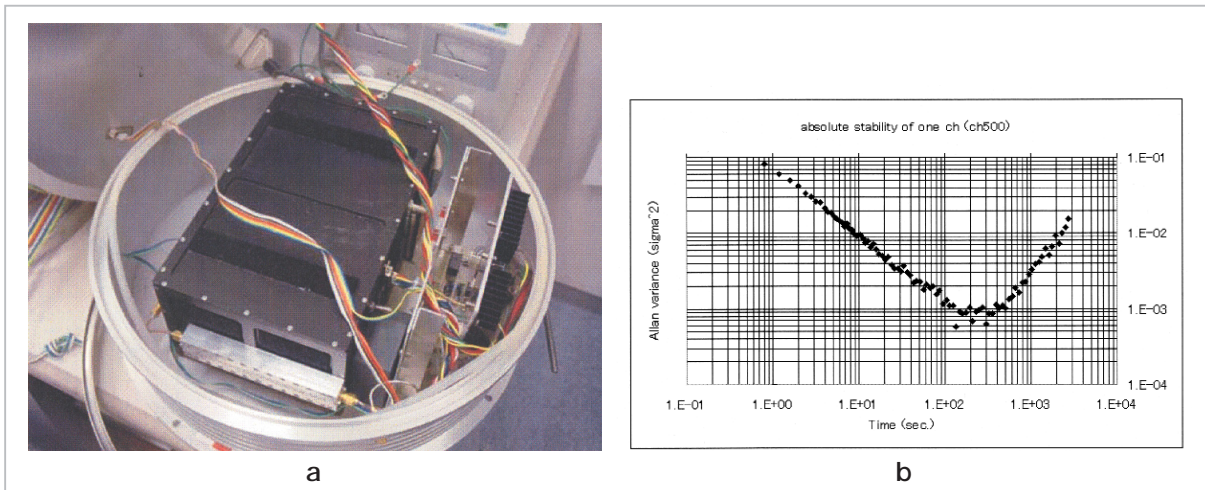


Fig.10 (a) Acousto-optical spectrometer, L 260 mm x W 125 mm x H 160 mm; (b) absolute stability of the Allan variance for the acousto-optical spectrometer

Table 1 Specifications for the acousto-optical spectrometer

Bandwidth	1 GHz(1.6-2.6 GHz)
Resolution	1.0 MHz
Number of channels	1728 pixel CCD
Integration time	17 msec. - 128 msec.
Light source	Laser diode 780 nm, monochrome, 50 mW
Type of diffraction grating	1 GHz Lithium Niobate Bragg cell, 90 ° polarization turning
Dynamic range	> 20 dB
Frequency error	< 2 MHz
Linearity error	< 0.1 %
Stability	Relative Allan variance > 200 sec.
Temperature stabilization	Laser Peltier stabilizer, AOS box Peltier stab., 4 sensors
Data acquisition	PC based software, plug in 32 bit fast I/O board
Power consumption	60 W warm up (10 min), 20 W steady state
Physical dimensions	L 260 x W 125 x H 160 mm
Weight	5 kg
Operational temperature range	0 to 40

scope; and (iii) an analog input board to acquire attitude data from an accelerometer as well as antenna-position data (stepping-motor address data) from CPU 2. The data of attitude and antenna position are acquired with a preset delay time after acquiring the 100-millisecond molecular spectrum data. For a delay time of 50 milliseconds, it takes about 150 milliseconds to acquire molecular spectrum data, attitude and antenna position data, and time data. We will acquire such a data set at a number of altitudes. The acquired data are recorded on a PC card attached to the CPU 1 unit. Since the card has a recording capacity

of 1.2 GB, given a data set of 7 kB it will be filled with data in about 7 or 8 hours following initial acquisition. The telemetric rate is 32 kbps at the fastest, which is too slow to relay all of the data to earth. Therefore the CPU units will be recovered after the gondola lands in the sea. It is necessary to ensure that the CPU units are waterproof and that they will not detach and sink on impact.

CPU 2 operates at a clock frequency of 33 MHz with a RAM of 4 MB under MS-DOS Version 5. The CPU 2 unit features the following boards, connected to an ISA bus: an analog I/O board (for the acquisition of HK

data, to monitor and control phase locking of local oscillators, and to control the output of the oscillator, and to switch to the comb generator signal), and a motor-controlling board (to control the stepping motor that drives the antenna). The HK data consist of temperature and voltage data for various components. The acquired data and time data are recorded in a 440-MB PC card attached to the CPU 2 unit, which will be recovered at sea. We expect to send the HK data to earth using a telemeter. In addition, CPU 2 will scan the antenna asynchronously with the acquisition of data from the spectrometer. Analog information on antenna position is sent as a stepping-motor address to CPU 1 (which acquires the information during the delay time). After recovery at sea, data of from the two CPUs will be collated using the recorded time data. A command can then be sent from earth to reset the CPUs. To prevent CPU-originated high-frequency noise from causing erroneous issuance of command system in the gondola, a metal container is used as a shield, noise filters are attached to connectors, and cases are carefully shielded. The data acquisition and control system could be slightly changed.

2.7 Detection of Attitude

To observe an altitude profile of trace gases in the stratosphere, it is necessary to determine the orientation of an observation beam with an accuracy of 0.1 degree. Since the gondola hangs from ropes connected to a balloon, the attitude of a gondola may not be stable. Some believe that it will prove stable in the stratosphere, although the gondola may swing slightly with gusts. Absolute stability in this case is not clear. Generally speaking, a gondola is said to swing like a pendulum, with a period between 20 seconds and 30 seconds. The movement of mirrors within the gondola may possibly add additional motion to the gondola. Assuming that the gondola swings with an amplitude of 0.5 degrees and a period of 20 seconds, this swing will not prove sufficient to scan an observation beam without moving the antenna, as the width and time of

such scan must be 12 degrees and 20 seconds, respectively. An attitude controller may be placed on board the gondola, but this has the drawback of adding extra weight (For astronomical observations, a flywheel is used to control the azimuth.). In this mission, we determined not to use an attitude controller, but instead placed an attitudinal detector on board. The gondola should rotate around the yaw axis (or azimuth axis) at a rate of 1 rpm. We assume that ozone and other trace molecules exist uniformly within a 550-km radius around the gondola and that integration of data is possible on a horizontal plane. As shown in Fig.11, the attitude detector features a fiber-optical gyroscope (as an angular velocity meter) and an accelerometer. Each of these meters features three mono-axial meters for use in combination as tri-axial meters. The angular resolution of the gyro is 0.01 degree with a minimum data transmission interval of 20 milliseconds. To maintain this level of accuracy, it will be necessary to conduct further experiments and studies on mounting precision, temperature stabilization, linearity, bias correction, and data calibration. Tables 2 and 3 show the specifications for a mono-axial fiber-optical gyroscope and a mono-axial accelerometer.

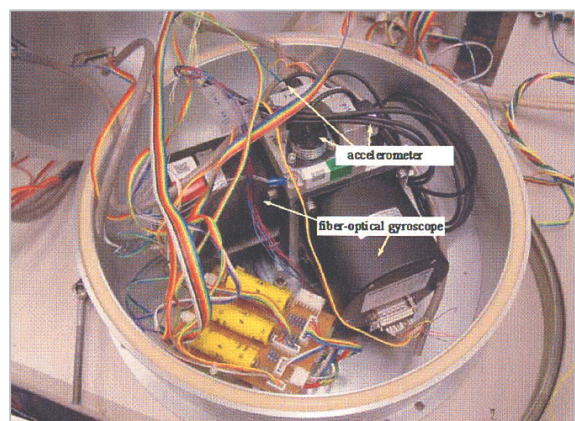


Fig. 11 Tri-axial fiber-optical gyroscope and accelerometer

2.8 Power Source

Primary lithium cells of a few Ah to 30 Ah are used as a power source. Based on the measured voltage and current of sub-systems,

Table 2 Specifications for a mono-axial fiber-optical gyroscope

Item	Unit	Rated value
Range of measurable angles	°	± 180
Range of measurable angular velocity	° /s	± 200
Resolution	Angle	0.01 or less
	Angular velocity	0.01 or less
Linearity †	%FS	± 0.1 or less
Bias stability ††	° /h	± 3 or less (over the entire range of operating temperatures)
Angular drift*	° /h	± 0.5 or less (to achieve a stable temperature T after bias correction)
Transmission rate	msec	Selected from 20, 50, 100, 200, 250, 500, and 1,000
Frequency response	Hz	Depends on the transmission rate
Misalignment**	mrad	7 or less
Operating temperature		- 10 to + 50
Storage temperature		- 20 to + 60
Vibration	m/s ²	49(20Hz to 200Hz)
	G	5(20Hz to 200Hz)
Impact	m/s ²	196(11 ms)
	G	20(11 ms)
Humidity	%RH	85 or less. No dew is allowable
Power voltage	VDC	11 to 16(with a built-in DC-DC converter)
Current consumption	A	1.0 or less

When a low-pass filter (10 Hz or less) is connected, it should be possible to read the above angular velocity

† Linearity: Linearity of output for an input angular velocity or an input angle, including non-linearity, asymmetry, and temperature stability of the scale factor

†† Bias stability: Bias (angular drift) stability over the entire range of operating temperatures, within a temperature variation of 0.5 degrees/min or less

* Angular drift: Angular drift at a stabilized temperature after bias correction

** Misalignment: Slope of the input axis against the mounting reference plane

Table 3 Specifications for a mono-axial accelerometer

Item	Unit	Rated value
Measurement range (F.S)	m/s ²	± 29.4
	G	± 3
Sensitivity	V/(m/s ²)	0.204 ± 5%
	V/G	2.000 ± 5%
Resolution	m/s ²	4.9×10 ⁻⁵ or less
	G	5 × 10 ⁻⁶ or less
Linearity (to F.S)	%	± 0.10 or less
Frequency response(± 3 dB)	Hz	DC to 250 or more
Zero point imbalance ¹⁾	m/s ²	Within ± 0.98
	mG	Within ± 100
Case alignment	°	± 0.5 or less
Sensitivity in transverse direction ²⁾	%	0.5 or less
Temperature coefficient of sensitivity ³⁾	%/	0.03 or less
Temperature coefficient of zero point ⁴⁾	(m/s ²)/	± 2.94×10 ⁻³ or less
	μ G/	± 300 or less
Power voltage	VDC	± 11 to ± 16(± 15: nominal value)
Current consumption		18mA+3mA/(9.8 m/s ²)(nominal value)

Operating temperature range		- 25 to + 70 or less
Coefficient of zero point power voltage	(9.8 m/s ²)/V	9.8 × 10 ⁻³ or less
	G/V	1 × 10 ⁻³ or less
Coefficient of sensitivity power voltage	%/V	0.1 or less
Range of storage temperature		- 40 to + 80
Vibration	m/s ²	2.0 × 10 ² (at 25 Hz to 1,000 Hz, in the tri-axial directions)
	G	20(at 25 Hz to 1,000 Hz, in the tri-axial directions)
Impact	m/s ²	9.8 × 10 ² (11 msec semi-sine wave, in hex-axial directions)
	G	100 (11 msec semi-sine wave, in axial-axial directions)

- 1) Zero point imbalance: Output due to torque caused mainly by a deviation in position of the mechanical zero point, regardless of input acceleration
- 2) Sensitivity in transverse direction: Change in voltage caused by applying acceleration along the axis of rotation of a pendulum, expressed in terms of percentage of a sensitivity voltage
- 3) Temperature coefficient of sensitivity: Dependence of sensitivity on temperature, with a reference state at 25
- 4) Temperature coefficient of zero point: Dependence of zero-point imbalance on temperature, with a reference state at 25

a power supply is prepared as a series and parallel combination of cells. Considering that the voltage decreases with a decrease in ambient temperature, suitable combinations should be designed. Since a three-terminal regulator is used to stabilize the voltage, it is necessary to determine the voltage such that it does not fall below the required minimum input voltage at low temperatures under the applied load. Experiments have revealed that the ambient temperature remains at approximately 0 in a thermally insulating polystyrene box when placed within a gondola (expectedly at - 20) in the space at - 50 . However, we must conduct experiments to determine the temperature of the cells in a vacuum-chamber test. The duration of observation is approximately 5 hours, and the total time is 10 hours, including preliminary time. In further consideration of testing times and the required margin of spare time, retention time was designed to be 20 hours. Heat generated by the regulator depends on current consumption and on the difference between input and output voltage. This heat will be released to heat sinks, such as the pressurized chamber and the gondola itself.

2.9 Pressurized Chamber and Temperature Control

As shown in Fig.12, the pressurized chamber features IF systems, a PLL circuit, a spec-

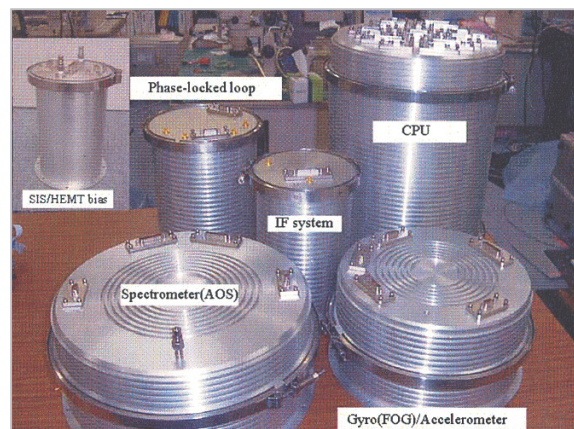


Fig.12 Pressurized chambers for a water-proof, heat-dissipating, noise-shielding, and for operation in a vacuum environment

trimeter, CPUs, a gyro, an accelerometer, and SIS/HEMT bias circuits. It serves as a noise shield for CPUs and for vacuum operation of the CPUs, IF systems, and bias circuits. Air in this chamber is to be replaced by dry nitrogen gas. However, pressurized chambers containing devices (such as the CPU, IF system, and bias) are filled with nitrogen gas containing a sufficiently low level of moisture to prevent the formation of dew. In a leak test with ambient air at 3 torr (equivalent to a vacuum at an altitude of 35 km) for 20 hours, a pressurized chamber for an IF system was kept at one atmosphere for 20 hours. In another test, pressurized chambers for the CPU and bias were evacuated and found to maintain a vacuum of several torr for 24 hours. In a test with

a pressurized chamber for an IF system, the chamber was kept filled with air at 25 °C, and the temperature of the system devices was measured at 40 °C. The chamber was then placed on a surface at 0 °C; the device temperature then fell to 15 °C at one atmosphere. In this case, the chamber was evacuated to 4 torr (0.53 kPa), and the device temperature increased by 10 degrees to 25 °C. Thus, we found that the device temperature changes along with a change in temperature of the contact surface (of the gondola) and increases with an decrease in the pressure of the chamber. Since the gondola's temperature, however, is not controlled by any device, the temperature within the chamber will be determined by the gondola's temperature which will be determined by the ambient temperature and by the amount of heat generated by other devices. Thus, it is important how to place the pressurized chambers within the gondola. Perfect thermal insulation may cause the devices to be heated above the operable temperature range. On the other hand, attaching a chamber to a heat sink that is too cold may cause the temperature to fall below the required range. The ambient temperature at an altitude of 35 km is said to be -50 °C; the temperature of the gondola may be higher. During daytime observation, the chambers may be heated by the sun. While the gondola passes through low-temperature zones (at -80 °C, for example), it may need to be kept warm. We should conduct

experiments to determine the way of placing pressurized chambers.

3 Conclusions

A balloon-borne superconducting submillimeter-wave limb-emission sounder (BSMILES) is being developed for observations of the global atmosphere. This development has proceeded in conjunction with the development of a submillimeter-wave band receiver, and with improvements in performance of the latter, will have a significant impact on related areas in radio astronomy. Development of such a receiver will thus represent a preliminary step toward similar observation from space.

BSMILES will be subject to a variety of tests at low temperatures and in vacuum, with a view to a scheduled launch in 2003. After successful observations, the relevant instruments will be recovered at sea, and data analysis will begin. We plan to configure these instruments to observe more types of molecules and to perform a series of observation runs. We also have plans to apply BSMILES to verification of the performance of JEM/SMILES_[14]. Table 4 shows an estimation of the weight and power consumption of BSMILES. Table 5 shows the specifications for the BSMILES instruments and observation procedures.

Table 4 Estimation of the weight and power consumption of BSMILES

Weight in kg					
Gondola	Antenna system	Optics system	Liquid helium tank	Phase-locked loop (PLL)	Intermediate frequency (IF) system
70	27	28	35	12	10
Spectrometer	PC	Attitude system	Telemetry system	Ballast	Total
20	23	15	60	120	420

Power consumption in watts							
Drive system	Receiver	PLL	IF system	Spectrometer	PC	Attitude system	Total
20	0.1	22	26	20(60)	31	23	142(182)

Table 5 Specifications for BSMILES instruments and observation procedures

Specifications for the instruments	
Gondola	Dimensions: L1.35 m × W1.35 m × H1.26 m
Antenna	Offset parabolic antenna (300 mm in aperture and 0.1 degree in beam size, fixed), sub-reflector, and flat mirror (630 mm × 350 mm) for beam scanning
Optics system	Standing wave reducer, Martin Puplett interferometer-type SSB filter, cold-load image terminator, focusing mirrors, wire grid for LO injection, and phase lock submillimeter-wave oscillator
Receiver system	650-GHz band SIS mixer ($T_{rx}(DSB) = 150$ to 200 K), and HEMT amplifier (5 to 7 GHz, $T_e = 18$ K)
Calibration system	Flat mirror for calibration and calibrated hot load
IF system	Amplifiers, power divider, combining amplifier, filters, etc.
Spectrometer	Acousto-optical spectrometer with a bandwidth of 1 GHz and resolution of 1 MHz
Data acquisition and control system	CPU1: acquisition of molecular spectrum data, attitude data, and antenna position data, connected to a 1.2-GB ATA flash PC card CPU2: acquisition of HK data, control of antennas and the comb generator signal switch, monitoring and auto-control of oscillator phase locks and power
Attitude detection system	Tri-axial fiber-optical gyroscope with an angular resolution of 0.01 degree, tri-axial accelerator
Power source	Primary lithium cells, three-terminal regulator
Telemetry	Maximum transfer rate: 32 kbps
Weight	Approximately 420 kg, including ballast of 120 kg
Power consumption	Approximately 140 W
Other	Pressurized chambers (waterproof, shielded, etc.): No attitude control; equipment to be recovered at sea and reused.

Specifications for observation procedures

Molecules to be observed	O ₃ , ClO, HO ₂
Observation frequency band (band width)	ClO : 649.450GHz, HO ₂ : 649.701GHz (500 MHz) O ₃ : 650.733GHz (500 MHz)
Altitude of observation	10 to 35 km
Altitude resolution	Approximately 1 km
Measurement accuracy	Approximately 10 percent
Observation time	Approximately 5 hours
Place and time of balloon launch	Sanriku, 2003

References

- 1 J. W. Waters, J. C. Hardy, R. F. Jarnot, H. M. Pickett, and P. Zimmermann, "A Balloon-borne Microwave Limb Sounder for Stratospheric Measurements", *Journal of Quantitative Spectroscopy & Radiative Transfer*, Vol. 32, No. 5/6, pp.407-433, 1984.
- 2 J. W. Waters, R. A. Stachnik, J. C. Hardy, and R. F. Jarnot, "ClO and O₃ Stratospheric Profiles: Balloon Microwave Measurements", *Geophysical Research Letters*, Vol. 15, pp.780-783, Aug. 1988.
- 3 A. Dechamps, P. Encrenaz, P. Feuvre, H. G. Floren, S. George, B. Lecomte, B. Ljung, L. Notdh, G. Olofsson, L. Pagani, J. R. Pardo, I. Peron, M. Sjokvist, K. Stegner, L. Stenmark, J. Tauber, and C. Ullberg, "Results of the PIROG 8 Balloon Flight with an Embarked Experiment Based on a 425/441 GHz SIS Receiver for O₂ Search", *Ninth Int. Symposium of Space Terahertz Technology*, pp.253-

261, Pasadena CA, Mar. 1998.

- 4 J. R. Pardo, L. Pagani, G. Olofsson, P. Febvre, and J. Tauber, "Balloon-borne Submillimeter Observations of Upper Stratospheric O₂ and O₃", *Journal of Quantitative Spectroscopy & Radiative Transfer*, Vol. 67, pp.169-180, 2000.
- 5 R. A. Stachnik, J. C. Hardy, J. A. Tarsala, J. W. Waters, and N. R. Erickson, "Submillimeterwave Heterodyne Measurements of Stratospheric ClO, HCl, O₃, and HO₂: First Results", *Geophysical Research Letters*, Vol. 19, No. 19, pp.1931-1934, Oct. 2, 1992.
- 6 J. Mees, S. Crewell, H. Nett, G. de Lange, H. van de Stadt, J. J. Kuipers, and R. A. Panhuyzen, "ASUR - An Airborne SIS Receiver for Atmospheric Measurements of Trace Gases at 625 to 760 GHz", *IEEE Transactions on Microwave Theory and Technologies*, Vol. 43, No. 11, Nov. 1995.
- 7 J. Urban et al., "Recent Airborne Heterodyne Receivers for the Submillimeter-wave Range", *International Workshop on Submm-wave Observation of Earth's Atmosphere from Space*, pp.1-13, Jan. 1999.
- 8 M. Okabayashi, M. Taguchi, S. Okano, and H. Fukunishi, "Observation of Upper Stratospheric Ozone by Balloon-Borne Optical Ozonesondes", *The Institute of Space and Astronautical Science Report SP, No.32*, Mar. 1995.
- 9 K. Hitsuda, T. Toriyama, Y. Matsumi, and Y. Kondo, "Development of Balloon-Borne Instrument for Measurement of ClO - Optimization of System and Design of Gondola -", *10th Symposium of Atmospheric Chemistry*, 2000.
- 10 Y. Irimajiri, T. Noguchi, S.-C. Shi, T. Manabe, S. Ochiai, and H. Masuko, "A 650-GHz Band SIS Receiver for Balloon-Borne Limb-Emission Sounder", *Int. J. of Infrared and Millimeter Waves*, Vol. 21, No. 4, pp. 519-526, Apr. 2000.
- 11 J. Zmuidzinas, H. G. LeDuc, J. A. Stern, and S. R. Cypher, "Two-junction tuning circuits for submillimeter SIS mixers", *IEEE Trans. Microwave Theory Tech.*, Vol. 42, No. 4, pp. 698-706, Apr. 1994.
- 12 T. Noguchi, S. C. Shi, and J. Inatani, 'An SIS mixer using two junctions connected in parallel', *IEEE Trans. Applied Superconductivity*, Vol. 5, No. 2, pp. 2228-2231, Jun. 1995.
- 13 S. C. Shi, T. Noguchi, J. Inatani, Y. Irimajiri, and T. Saito, 'Experimental Results of SIS Mixers with Distributed Junction Arrays', *Ninth Int. Symp. on Space Terahertz Tech.*, Pasadena, CA, pp.223-234, Mar. 1998.
- 14 H. Masuko, S. Ochiai, Y. Irimajiri, J. Inatani, T. Noguchi, Y. Iida, N. Ikeda, and N. Tanioka, "A superconducting sub-millimeter-wave limb emission sounder (SMILES) on the Japanese Experimental Module (JEM) of the Space Station for observing trace gases in the middle atmosphere," *Eighth Int. Symp. Space Terahertz Technology*, pp.25-27, Harvard MA, Mar. 1997.



IRIMAJIRI Yoshihisa, Dr. Sci.

*Senior Researcher, SMILES Group,
Applied Research and Standards Division*

Development of Millimeter-and Submillimeter-Wave Receiver and System